

PRECIPITATION FROM VERTICAL MOTION: A STATISTICAL DIAGNOSTIC SCHEME

BRIAN E. J. ROSE and CHARLES A. LIN*

Department of Atmospheric and Oceanic Sciences, McGill University, Centre for Climate and Global Change Research, Centre de recherche en calcul appliqué, Montreal, Canada

Received 6 April 2002

Revised 15 March 2003

Accepted 21 March 2003

ABSTRACT

The relationship between precipitation and atmospheric vertical motion is investigated over the globe. By combining and averaging precipitation rates within small ranges of vertical motion, the mean precipitation rate is found to vary smoothly with vertical motion. The relationship is modelled with a simple function that assumes zero precipitation for subsidence and linearly increasing precipitation for ascending motion. Function parameters are computed from National Centers for Environmental Prediction reanalysis data individually for every grid point and calendar month. Variations in the slope account for geographical and seasonal variations in moisture and other precipitation factors. At each grid point, the scheme diagnoses precipitation rate from a single concurrent value of vertical motion. It is shown to have moderate skill over climatology in predicting mean monthly precipitation. The midlatitudes, oceans and the winter season are favoured. The scheme is designed to extract precipitation fields from a dry general circulation model, based on the simulated vertical motion. Application to climate modelling is discussed. Copyright © 2003 Royal Meteorological Society.

KEY WORDS: global; precipitation; vertical motion; diagnostic scheme; climate

1. INTRODUCTION

The phenomenon of precipitation may epitomize the challenge faced by all Earth scientists. To the layperson it is simple and familiar; to the 'expert' it is a baffling mystery. Like a fractal pattern, the closer we look the more complicated it becomes. This paper represents a modest effort to step back and exploit a simple but physically based concept for precipitation in the context of climate modelling.

It is reasonable to expect some correlation between precipitation and atmospheric vertical motion, for the simple reason that updrafts drive the condensation process. Vertical motion measured on a coarse-scale grid characteristic of a general circulation model (GCM) can be considered a measure of the synoptic-scale forcing for ascent and descent. To what extent is this forcing correlated with precipitation? In this paper we will illustrate an interesting relationship between these two variables using past climate data. We will develop a statistical diagnostic formula for precipitation using only vertical motion as a predictor, and provide some bounds on the expected skill of the technique. Although these results are interesting on their own, there is also a practical application.

Recently, Hall (2000) has developed a simple atmospheric GCM based on dry dynamics that provides a remarkably realistic climate at very low computational cost. Using the statistical methods developed in this paper, the vertical motion fields produced by Hall's model can be translated into precipitation fields, with no moisture information as input. This very efficient climate model could then be applied to different problems, such as seasonal prediction experiments and global rainfall response to climate perturbations.

*Correspondence to: Charles A. Lin, Department of Atmospheric and Oceanic Sciences, McGill University, 805 Sherbrooke Street West, Montreal, QC, H3A 2K6, Canada; e-mail: charles.lin@mcgill.ca

The search for a possible relation between precipitation and vertical motion is not new. For example, van den Dool (1987) used 3 years of data to show that anomalies in precipitation and vertical motion at 500 hPa are moderately correlated over the USA, especially in winter. In this study, we use a longer data set going back to 1948 over the globe to search for a statistical relation. Other studies have focused on a relation between precipitation and topographically forced vertical motion (Sinclair, 1994) or cyclonic activity (Chen *et al.*, 1997).

The rest of this paper is concerned with developing and validating the diagnostic precipitation scheme. Section 2 will introduce the data and show some simple correlations. Sections 3 and 4 form the core of the paper, where first a robust statistical relation between precipitation rate and vertical motion is documented, and then the diagnostic scheme is constructed. In Section 5 we attempt to quantify the uncertainty of the scheme by applying some objective skill measures. A summary and discussion of potential applications are given in Section 6.

2. DATA CHARACTERISTICS

2.1. Data sources

Vertical motion and precipitation data are taken from the National Centers for Environmental Prediction (NCEP) reanalysis, a global assimilation and analysis of rawinsonde data, surface synoptic data and secondary sources, from 1948 through to the present (Kalnay *et al.*, 1996). The fields are available at a temporal resolution of 6 h. We have chosen to use this data set by virtue of its unparalleled long time span, global coverage and sub-synoptic temporal resolution. However, the validity of the data (in particular the precipitation) may be questioned. Kalnay *et al.* (1996: 448) designate the reanalysis vertical motion as a 'B' variable, indicating that 'although there are observational data that directly affect the value of the variable, the model also has a very strong influence on the analysis value...'. By contrast, the precipitation rate is a forecast value, entirely generated by the reanalysis model, which is a 'C' variable (Kalnay *et al.*, 1996). No observations of precipitation are assimilated. Therefore, one must exercise caution in attributing features of the data to the real climate. However, the fields appear to be quite realistic in the extratropics; see Janowiak *et al.* (1998) for a detailed study of the reanalysis precipitation.

Some verification of results will be performed with a precipitation data set derived from observations, the Global Precipitation Climatology Project One-Degree Daily product (hereafter referred to as 1DD); see Huffman *et al.* (2001) for details. This data set, and its parent monthly precipitation data set (Huffman *et al.*, 1997), result from a global analysis of a very large number of rain gauge observations, blended with various satellite-based precipitation estimates. The blending of different data sources allows for a total global best estimate of precipitation. The 1DD data set spans 1997 through to the near present.

2.2. Correlations between precipitation and vertical motion

The vertical motion data are available on 12 pressure levels. One might expect precipitation to be best correlated with vertical motion somewhere in the mid to lower troposphere. Standard correlation coefficients between precipitation rate and vertical motion were computed with respect to time over one year (1996) and averaged over latitude and longitude. Figure 1 shows the average correlation with respect to pressure level, computed for the whole globe and separately for various latitude bands. There is a broad peak in negative correlation in the lower middle troposphere. The correlation is negative as vertical motion is measured by the vertical pressure velocity, in pressure coordinates. The global curve has a maximum at 700 hPa, and none of the other curves shows a significant deviation from the 700 hPa peak. Based on this result, vertical motion values are taken exclusively at 700 hPa for the remainder of this paper.

A map of this same temporal correlation coefficient (Figure 2) reveals strong spatial variations in correlation. The highest correlation is seen over the midlatitude oceans, ranging from -0.5 to -0.8 . Correlation is a little lower over the continents, and much weaker throughout the tropics, between about -0.1 and -0.5 over most of the tropical Atlantic and Pacific basins. The lowest correlation (near zero) is found over most of continental

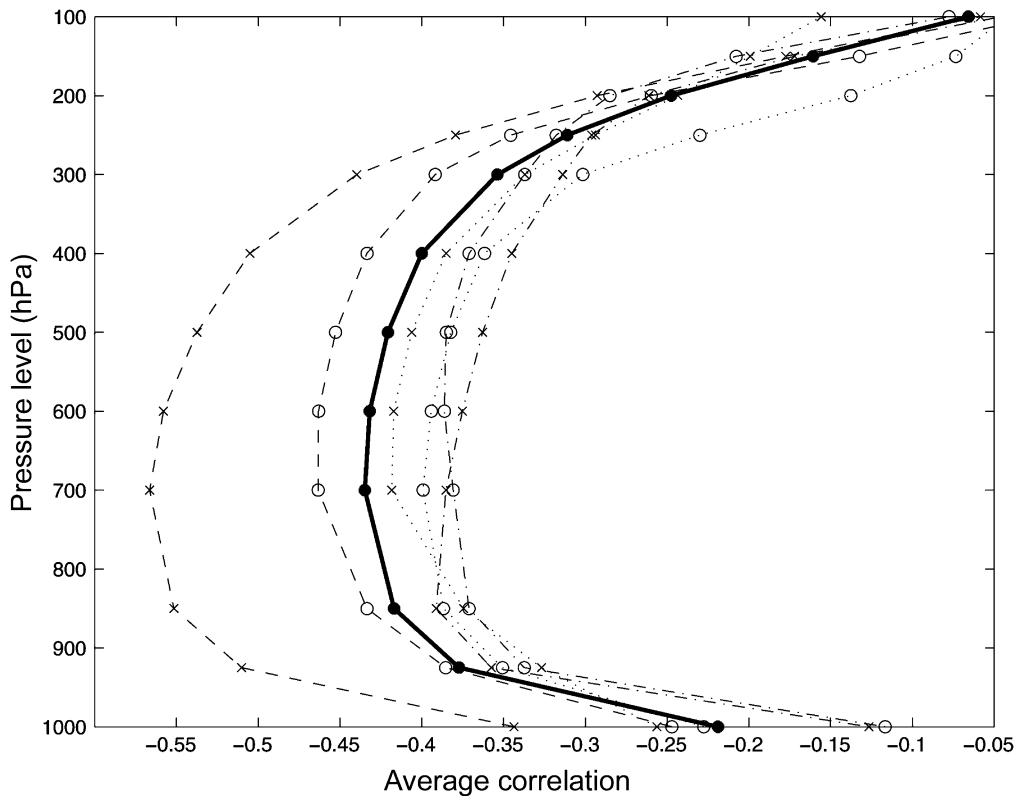


Figure 1. Average temporal correlation between precipitation rate over 1996 and vertical motion on each of 12 pressure levels. The solid curve represents the whole globe. Dotted curves are the high latitudes (60 to 90°) only, dashed curves are the midlatitudes (30 to 60°) only, and dot-dash curves are the tropical latitudes (0 to 30°) only. Circles represent the Northern Hemisphere and crosses represent the Southern Hemisphere

Africa and the west coast of South America. Correlation is consistently low over the very dry areas of the Earth. In these cases the precipitation is likely to be far better correlated with available moisture than with vertical motion. The same correlation map computed from 1DD rather than reanalysis precipitation data (not shown) reveals a similar distribution of high and low correlation.

Spatial correlation coefficients between precipitation and vertical motion were computed over zonal bands and plotted as time series in Figure 3. A seasonal oscillation in correlation is revealed for the midlatitudes. Correlation is highest in the winter season. The variation is more pronounced in the Northern Hemisphere, where winter correlation is near -0.55 , but summer correlation is only about -0.3 . These results indicate there is a reasonable to good correlation between our two variables of interest, thus motivating a more detailed examination in the next two sections.

3. JOINT VARIATIONS IN PRECIPITATION AND VERTICAL MOTION

Precipitation rate is highly variable; thus, its relationship to vertical motion is not simple. This relation is also expected to be significantly non-linear, since precipitation is often zero. In order to employ vertical motion as a predictor for precipitation, we need to identify systematic variations in the probability distribution of precipitation with vertical motion. These can be sought in the data according to the following procedure; for brevity we will call vertical motion ω , and precipitation rate p_{rate} .

We take a large set of paired $(\omega, p_{\text{rate}})$ data and sort them into discrete bins for small intervals of ω . The precipitation data in each bin is then treated as a random sample drawn from a population corresponding to

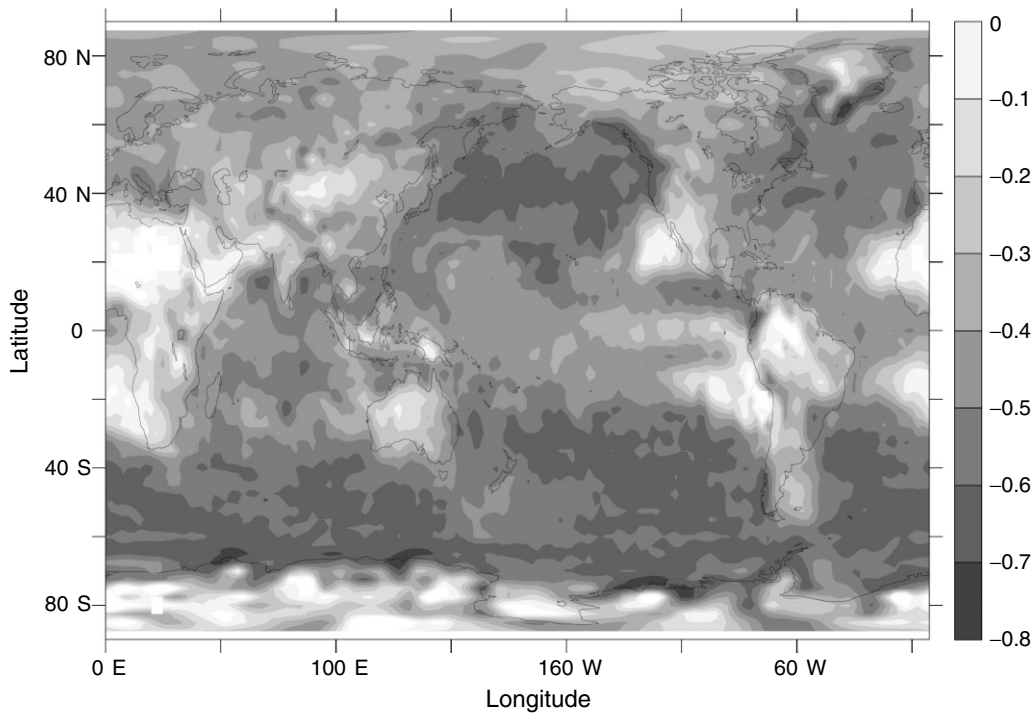


Figure 2. Temporal correlation between precipitation rate and vertical motion at 700 hPa, over 1996. Darker shading indicates stronger (negative) correlation

some ω within that interval. We choose arbitrarily the midpoint of the bin as the reference ω value; the bins are made narrow enough that this choice will not noticeably bias the results. We can then examine how the shape of the precipitation distribution changes with ω , e.g. by plotting frequency histograms of p_{rate} for each ω bin.

This procedure was applied to a set of paired (ω , p_{rate}) data over 5 years (1994–98) for all longitudes at 45° N. These data were sorted into 20 bins of negative (upward) ω . Positive ω data points (downward motion) were discarded, as they are not correlated with precipitation. Figure 4 shows frequency histograms of p_{rate} for each of these 20 bins. For large negative ω values (the top panels) the precipitation rate is widely distributed with a broad peak. As ω approaches zero the weight of the p_{rate} distribution shifts towards zero. Physically, this means that decreasing upward motion is associated with decreasing precipitation.

In Figure 5 the mean precipitation rate from each bin is plotted against their representative ω values. The linearity of the curve is striking. Since the sample mean is the best estimator of the underlying population mean, this result suggests that the expected value of precipitation rate increases linearly with negative vertical motion. Individual realizations of p_{rate} at a given ω will average out to this expected value.

A similar analysis was performed systematically for the whole globe. For every latitude, paired (ω , p_{rate}) data from all longitudes were combined into an ensemble. Precipitation rates (again from 1994 to 1998) were sorted by vertical motion into 70 bins of width 0.01 Pa/s with limits -0.4 Pa/s and 0.3 Pa/s. Mean precipitation was computed for each bin. Plots analogous to Figure 5 can then be drawn for each latitude; six representative plots are shown in Figure 6. The results are remarkably consistent and smooth: the mean precipitation rate curve is very nearly linear for negative ω , and very nearly zero for positive ω . The shape of the curve is consistent over the globe; only the slope varies with latitude. This is good evidence that the system exhibits some statistical regularity, which can be exploited for the purposes of developing a prediction scheme.

First, however, we must verify that this quasi-linear dependence of mean precipitation rate on vertical motion is a feature of the real climate and not an artifact of a model-generated data set. The same sorting and

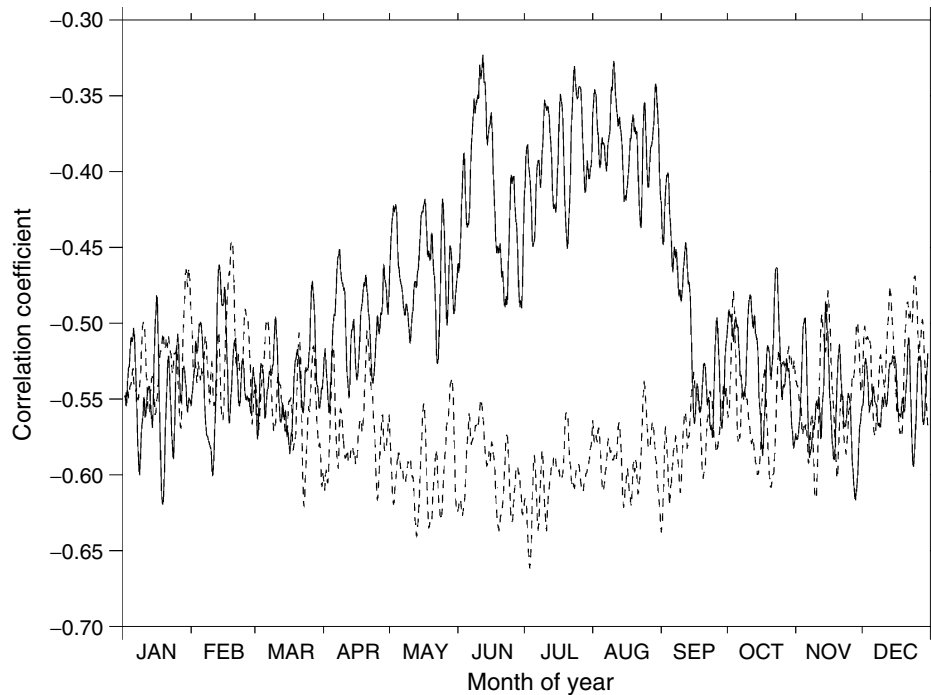


Figure 3. Time series of spatial correlation between vertical motion at 700 hPa and precipitation rate, smoothed with an eight-point (2 day) running mean. Solid curve is for northern midlatitudes (30–60 N) and dashed curve is for southern midlatitudes (30–60 S)

averaging procedure that was applied to reanalysis precipitation above can be applied to the observed IDD precipitation data. In Figure 7 the mean IDD precipitation is plotted against ω , again for six representative latitudes. The results are nearly identical to those for the reanalysis precipitation: mean precipitation rate is close to zero for positive ω , and increases nearly linearly with increasingly negative ω . Again, the qualitative shape of the curve does not change with latitude. Thus, the IDD and NCEP reanalysis precipitation results are consistent with each other, and we can proceed with confidence using the reanalysis data.

4. DIAGNOSING PRECIPITATION FROM VERTICAL MOTION

4.1. A first try

We have shown that the mean precipitation rate at a given latitude varies linearly with upward vertical motion ($\omega < 0$), increasing from near zero precipitation at $\omega = 0$. This behaviour is robust across all latitudes, although the slope varies. On the basis of this result we are able to estimate precipitation rate from vertical motion at any point on the globe using the simple formula

$$P = a(\phi)\omega + b(\phi) \quad (1)$$

where p_{rate} is precipitation rate, and a and b are slope and intercept parameters that depend on latitude ϕ . The slope and intercept at each latitude are estimated from the p_{rate} versus ω data (e.g. the plots in Figure 6) by standard least-squares linear regression. Van den Dool (1987) used an equation similar to Equation (1) to examine the relation between precipitation and vertical motion. He did not allow for an explicit dependence for the slope parameter on latitude, as the focus of his study was the USA.

Figure 8(a) is a global map of average precipitation rate over the year 1993 from the NCEP reanalysis, and Figure 8(b) is the same map calculated from vertical motion using Equation (1). The simple linear

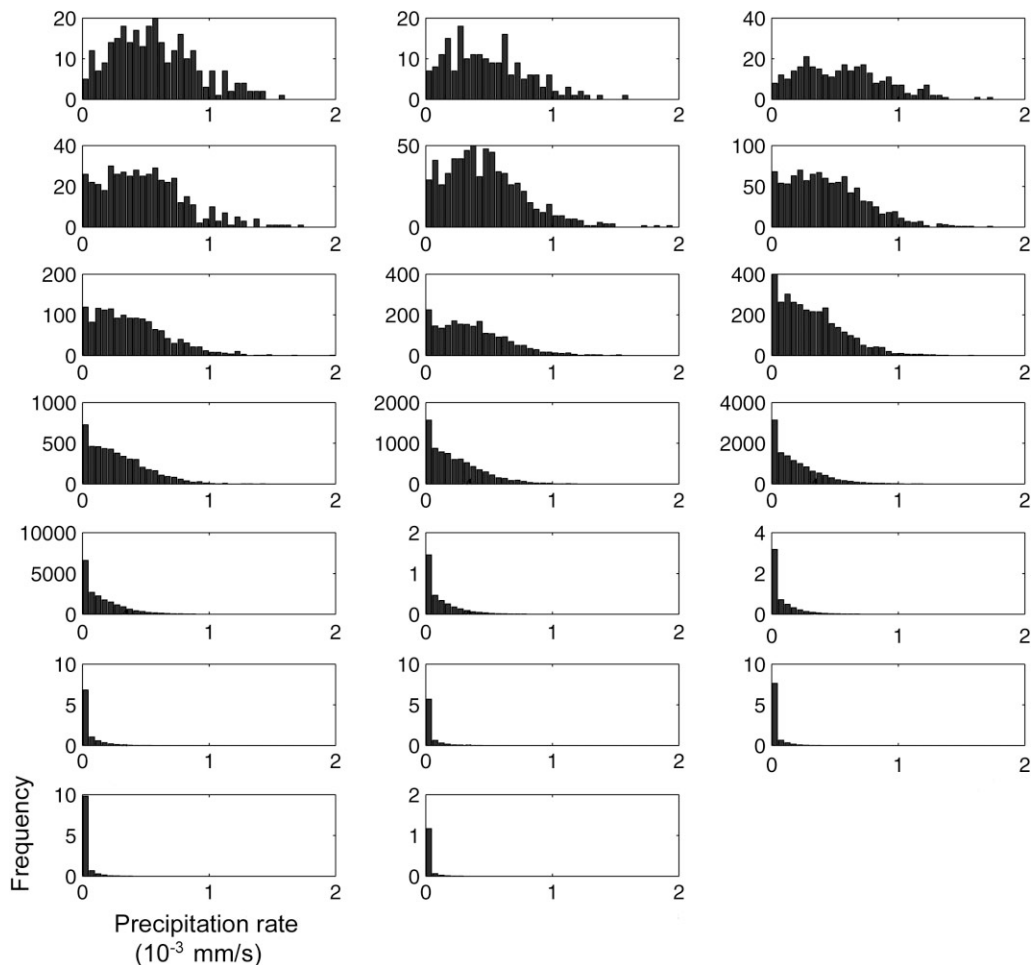


Figure 4. Frequency histograms of precipitation rate at 45°N (all longitudes) for 20 different vertical motion bins. Vertical motion ranges from strong upward motion ($\omega \leq -0.85$ Pa/s; top left panel) to weak upward motion (-0.025 Pa/s $< \omega < 0$; bottom right panel), reading from left to right and down the page

scheme gives a qualitatively correct picture of global annual precipitation, but the magnitudes are not very well represented. The precipitation in the dry desert areas is severely exaggerated, whereas the west Pacific/Indonesian precipitation maximum is substantially under-predicted, with the value of the peak only about half of what it should be. The predicted precipitation in the tropics shows an unrealistic tendency towards uniform zonal bands, which is a reflection of the regression parameters depending only on latitude.

Focusing on an individual grid point, Figure 9 shows a time series over 1993 of the 30 day running mean precipitation for the Montreal area in Quebec, Canada (about 45°N, 75°W). The solid and dashed curves correspond respectively to the NCEP reanalysis and the precipitation calculated from vertical motion using the present scheme, where the regression parameters depend only on latitude. The agreement is good, except over the summer period. The dotted curve corresponds to the rate obtained from the scheme used in Section 4.2 (OMEGA scheme).

These results suggest that the scheme works reasonably well for areas and seasons where precipitation tends to be forced by synoptic-scale systems (midlatitude winters especially). In the tropics, as well as during the summer in midlatitudes, convective precipitation is dominant. The associated vertical motions may be on scales much too small to be resolved in the coarse ω fields used here. Thus, the scheme is less successful for these times and regions.

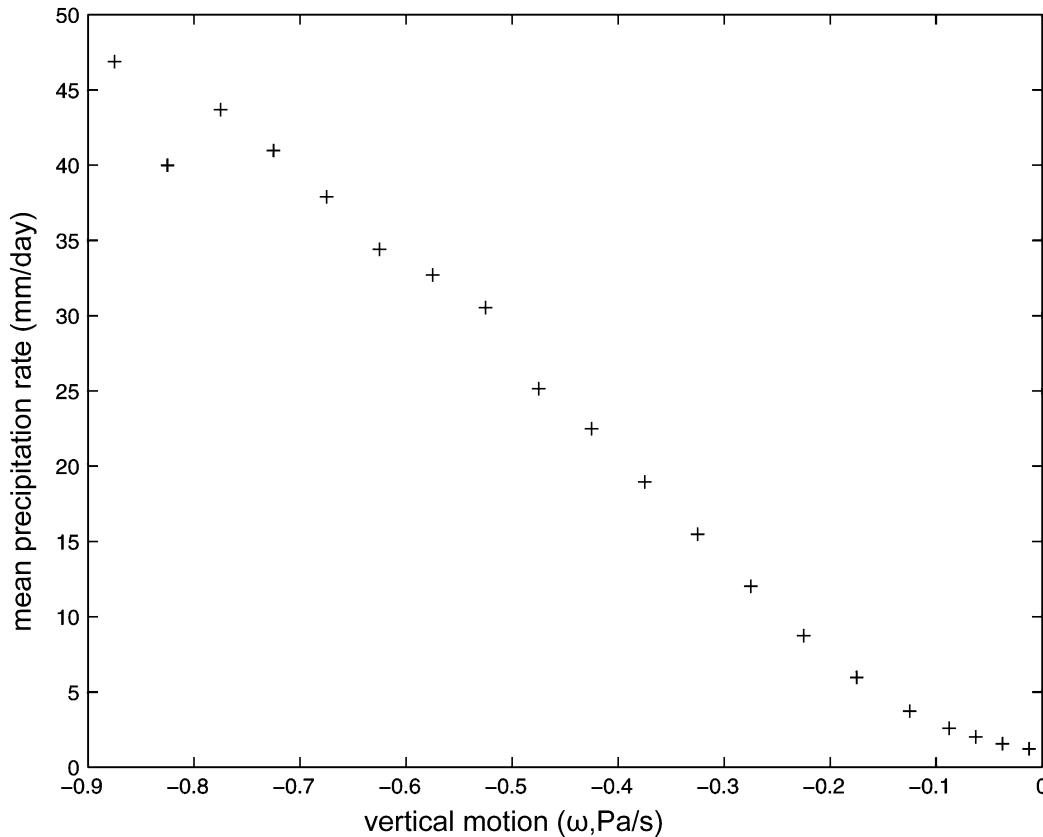


Figure 5. Mean precipitation rate for each vertical motion bin plotted against the midpoint value of the bin, based on the data shown in Figure 4

4.2. A second try

It is clear that there will always be uncertainty in a prediction of precipitation made without any measure of available moisture. Climatological moisture availability varies both geographically and seasonally; since the scheme described above depends only on latitude, it has only one degree of freedom with which to take account of these moisture variations. Therefore, it is expected that more accurate diagnoses of precipitation could be made by adding more degrees of freedom to the scheme. Van den Dool (1987) noted that the correlation between precipitation and vertical motion should vary with the moisture content of the atmosphere; in other words, the correlation should vary with season and location. We will attempt to take this variability into account by modifying our scheme as follows.

We now implement the simple regression scheme described earlier independently for every grid point and for each calendar month. NCEP reanalysis data for 12 years from 1976 through to 1987 at each grid point were divided into 12 monthly ensembles, and precipitation rates were sorted into bins according to their corresponding vertical motions. Straight lines were fitted to the mean precipitation rates for $\omega \leq 0$ as before. The results of the calculation are global fields of slopes and intercepts that depend on grid point location and calendar month. Using these new parameters, precipitation was computed from vertical motion over a 12 year verification period (1988 through to 1999). The formula is identical to Equation (1) except that the regression parameters (slopes and intercepts) are functions of latitude, longitude and calendar month. This method will be referred to as the OMEGA scheme. As noted earlier, the motivation for this scheme is to provide extra degrees of freedom in the statistical analysis to allow for the precipitation–vertical motion dependence on time of year and location (van den Dool, 1987).

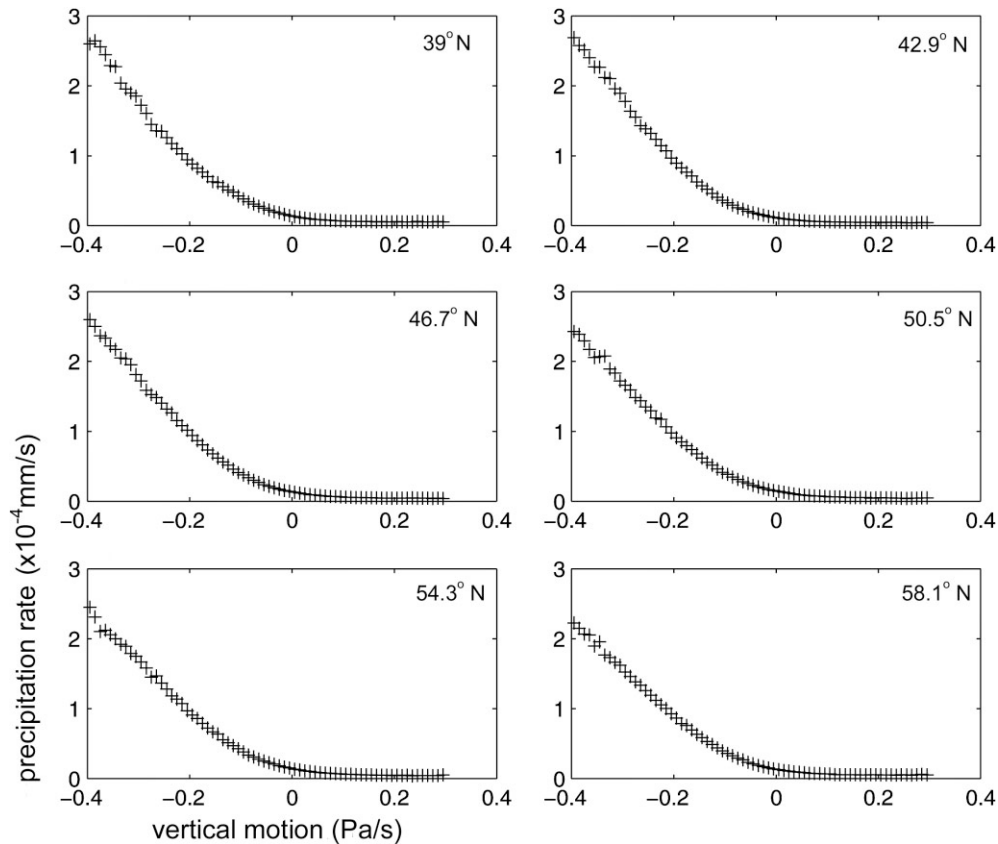


Figure 6. Some representative plots of mean precipitation rate (NCEP reanalysis) versus vertical motion bin. Each panel represents a latitude band

Figure 10 shows a map of the mean annual OMEGA precipitation rate over 1993. Compared with results of the earlier scheme shown in Figure 8, the improvements are clear: the desert areas are all well represented, the magnitude of the west Pacific maximum is much closer to the NCEP value, and the tropical precipitation no longer shows an unrealistic tendency towards zonal bands. Error is substantially reduced everywhere in general. Difference maps (not shown) reveal the error is very small over the deserts and throughout the midlatitudes.

Returning to the example of the Montreal grid point (Figure 9), the dotted curve shows the precipitation rate obtained from the OMEGA scheme. The improvement over the previous result is significant. The seasonal variability of the precipitation is now much better reproduced. Similarly good results have been obtained (figures not shown) for a grid point corresponding to Vancouver in western Canada. The extra degrees of freedom of the statistical scheme now allow for spatial and temporal discrimination.

5. SKILL STATISTICS OF THE OMEGA SCHEME

5.1. Definitions

The regression relation at the heart of the OMEGA scheme is designed to reproduce the mean expected precipitation for a given vertical motion. Given the large variability of precipitation rates, and the critical dependence on available moisture, OMEGA is not expected to resolve individual precipitation events accurately. Rather, it is hoped that OMEGA has some skill in reproducing the total (or average) precipitation

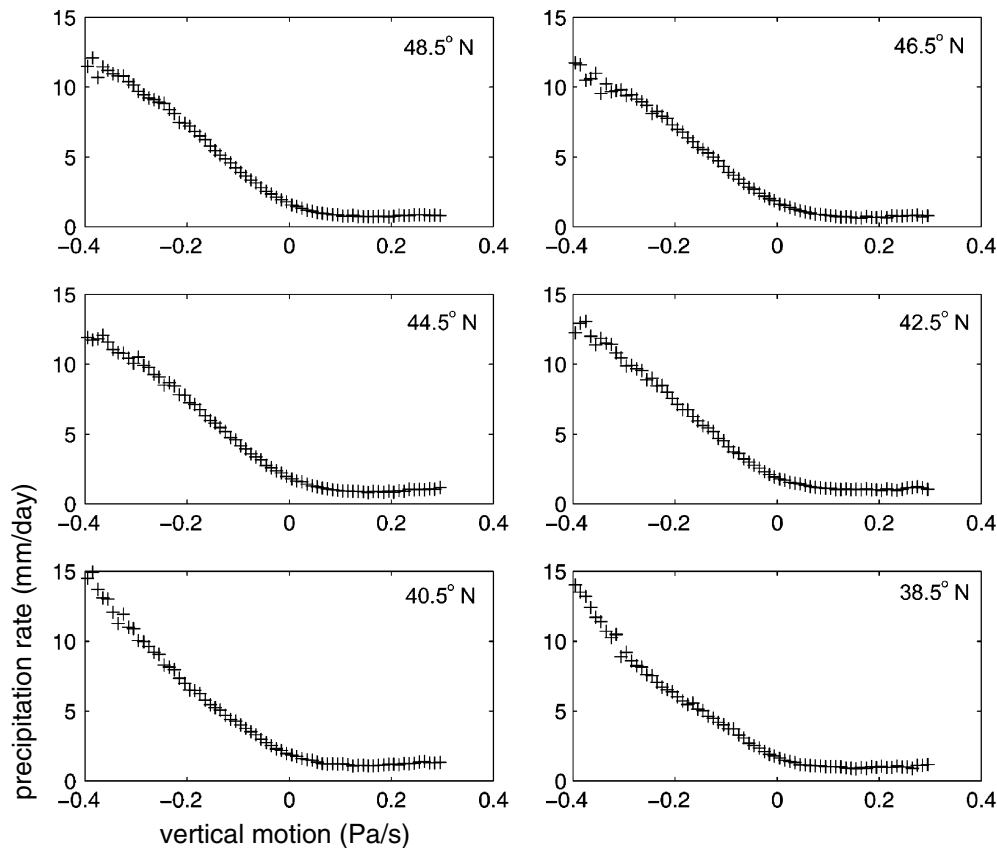


Figure 7. Some representative plots of mean GPCP IDD precipitation versus vertical motion bin for different latitude bands

over some climatological interval (a month, a season, a year, etc.). We focus on monthly precipitation totals, with the goal of reproducing the interannual variability over the 12 years' verification period (1988 through to 1999).

The skill of the OMEGA scheme will be measured against that of climatology using two simple statistics. The mean square error (MSE) skill score measures the skill of a forecast relative to a reference forecast, and is defined as (Wilks, 1995)

$$SS = 1 - \text{MSE}(\text{reference})/\text{MSE}(\text{forecast}) \quad (2)$$

where MSE is with respect to time. In this case, time is measured in months and the reference forecast is the monthly precipitation climatology. When defined this way, the MSE skill score gives a map of the forecast skill at each grid point, with a perfect forecast scoring unity and scores greater than zero indicating some skill over climatology.

As a skill measure for a forecast field at a particular time we will use the anomaly correlation coefficient (AC). This is simply the area-weighted correlation coefficient between forecast and observed fields, after subtracting climatology from both to get the anomaly fields. The AC of a forecast field is a single scalar, and taking the AC of successive fields over the verification period yields a time series of correlation coefficients. Positive correlation suggests forecast skill. The AC is designed to reward good forecasts of the spatial pattern of the observed field (Wilks, 1995). The subjective experience of operational forecasters suggests that $AC = 0.6$ is a reasonable threshold for distinguishing skilful forecasts (Wilks, 1995; von Storch and Zwiers, 1999).

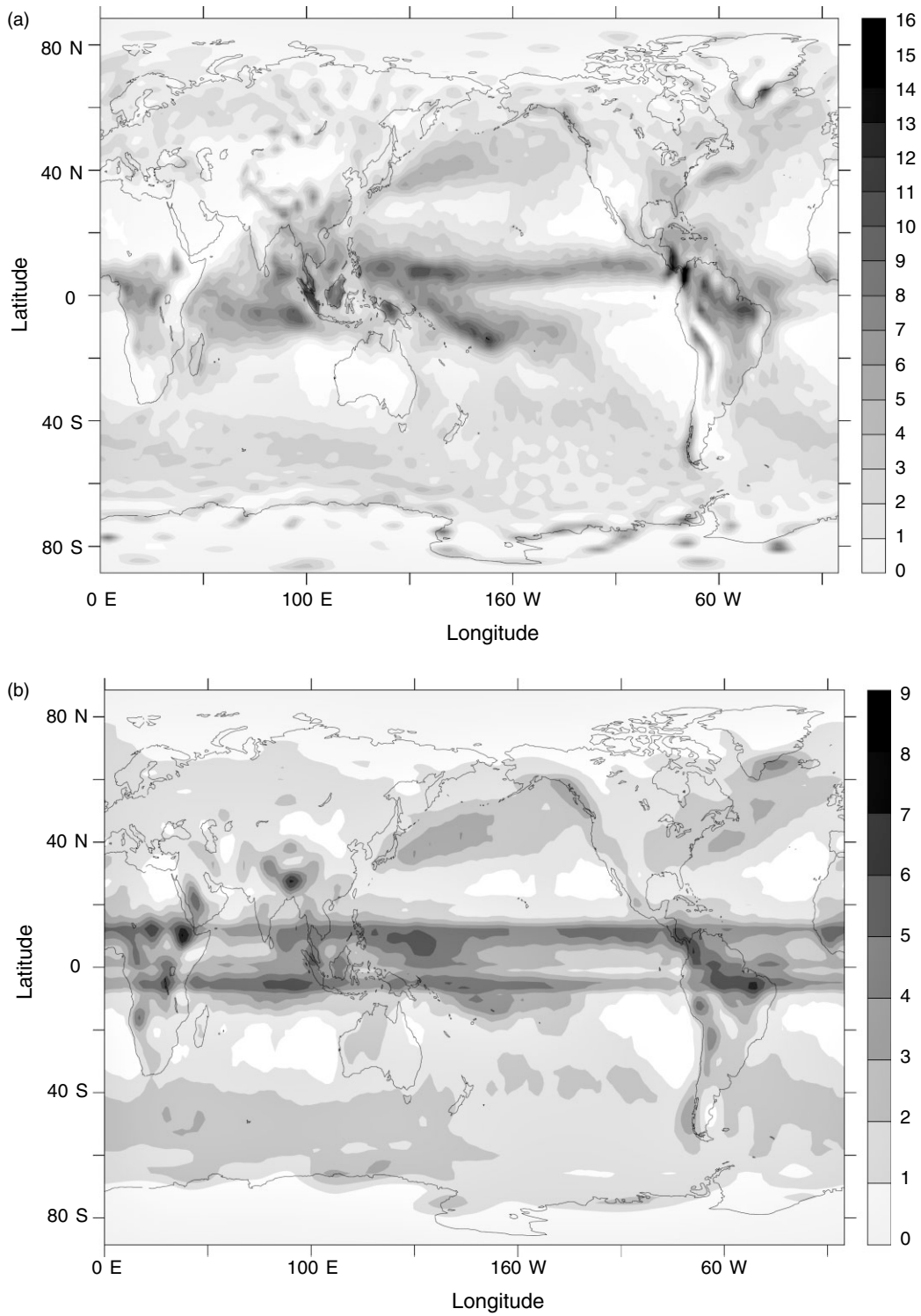


Figure 8. Mean annual precipitation rate over 1993 from (a) the NCEP reanalysis and (b) computed from vertical motion (units: mm/day). Darker shading indicates greater precipitation

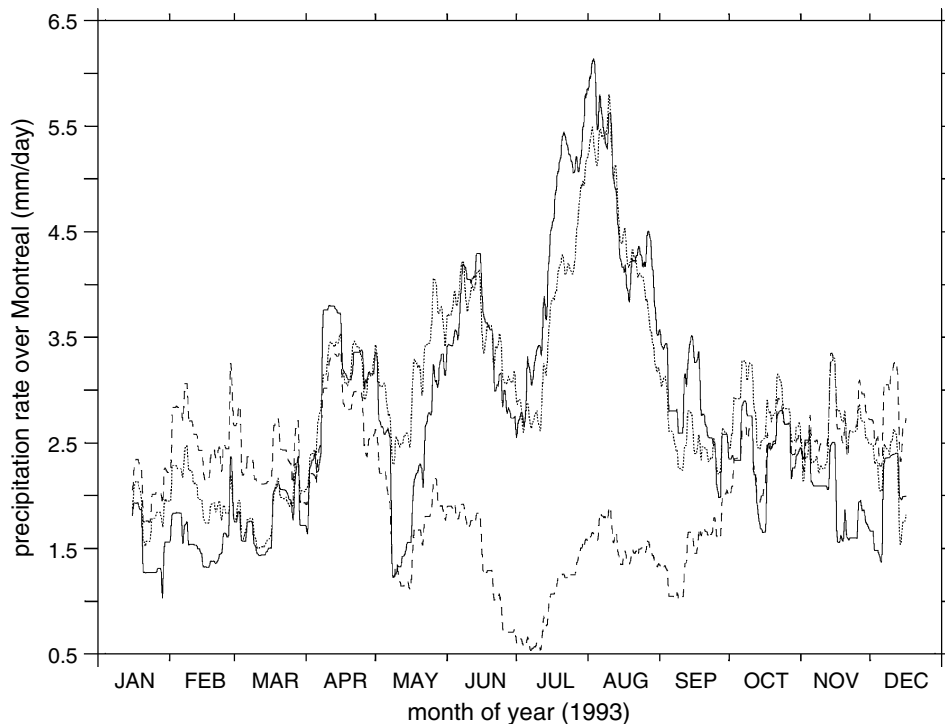


Figure 9. The 30 day running mean of precipitation rate at the grid point corresponding to the Montreal area. Solid curve is the NCEP reanalysis, dashed curve is computed from vertical motion with regression parameters depending only on latitude, and dotted curve is from the OMEGA scheme with regression parameters depending on longitude, latitude and calendar month

5.2. Results

Maps are plotted of the MSE skill score over the verification period (1988–99), with shaded areas indicating some skill over climatology, and darker shading indicating higher skill. Figure 11 shows the skill computed over the whole year and boreal winter (December–January–February) and summer (June–July–August) seasons. In this case, ‘climatology’ is the long-term mean precipitation for each month over the whole NCEP reanalysis time span (1948 to the present). In Figure 11 we see areas of positive skill over the oceans in midlatitudes as well as in the tropical western Pacific. Relatively large areas of negative skill exist in the tropical Atlantic, and along the equator off the west coast of South America. There is generally positive skill over eastern North America and Europe, and negative skill over Africa and much of Asia and South America. The highest skill can be seen along the west coasts of North America and Europe, as well as some parts of the southern Indian and Pacific Oceans. During boreal winter, very high positive skill can be seen along both coasts of North America, most of Europe and the eastern parts of the midlatitude Pacific Ocean. There is positive skill over almost all of midlatitude North America. In the Southern Hemisphere there are broad reaches of high skill over the midlatitude Oceans. In the Northern Hemisphere summer there is very little positive skill over the continents except for some improvement over South America. The area of high skill in the midlatitude north Pacific has shifted from east to west, extending eastward from Japan and Kamchatka.

Figure 12 shows plots of the AC over the 12 year verification period (1988–99) for the whole globe, and the northern (30–60 N) and southern (30–60 S) midlatitude bands. The subjective cut-off $AC = 0.6$ is included in the figure. Over the whole globe, the AC varies between about 0.30 and 0.55. Both the midlatitude time series show a clear annual signal (especially the Northern Hemisphere, where performance is poorest in the summer months). Performance is clearly superior in the midlatitudes; scores of over 0.6 are attained for several months of each year in both hemispheres. The Northern Hemisphere score varies between about 0.19

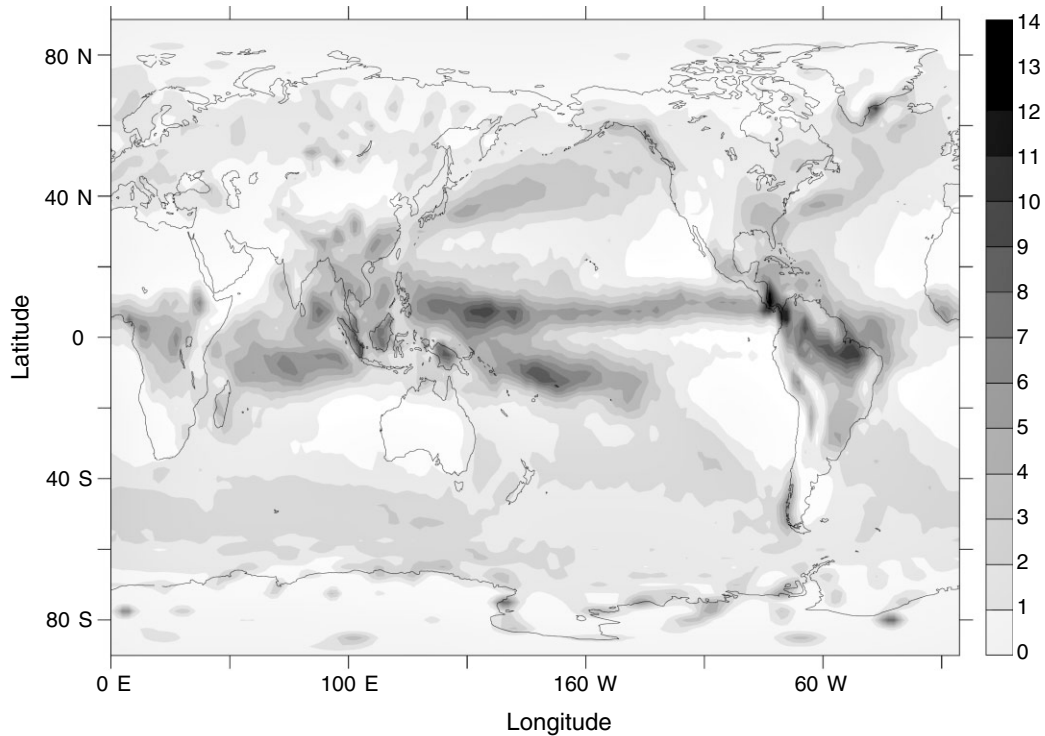


Figure 10. Mean annual precipitation rate over 1993 computed from vertical motion by the OMEGA scheme (units: mm/day). Darker shading indicates greater precipitation

and 0.71, and the Southern Hemisphere score varies between about 0.30 and 0.78. All three time series show a drop in performance from 1994 through to 1996.

The AC results are summarized in Table I, which lists mean values of AC over the 144 months, broken down by latitude band, and computed separately for land points and ocean points. The results are consistent with the earlier discussion: AC is highest in midlatitudes and lowest in the tropics, and, like the MSE scores, generally higher over the ocean than land. The highest mean AC (0.59) is found over ocean between 30 and 60 S; the lowest value (0.20) is found over land between the equator and 30 S.

5.3. Discussion

The OMEGA scheme has been tuned to reproduce the NCEP reanalysis precipitation fields using only one instantaneous measure of vertical motion as a predictor, with no direct information about moisture. Given

Table I. Mean AC scores over the 144 months of the 12 year verification period (1988–99), for different latitude bands and land/ocean grid points

	All points	Land only	Ocean only
All latitudes	0.42	0.32	0.45
90–60 N	0.49	0.50	0.48
60–30 N	0.51	0.50	0.55
30 N–0	0.38	0.28	0.40
0–30 S	0.37	0.20	0.42
30–60 S	0.57	0.41	0.59
60–90 S	0.55	0.55	0.55

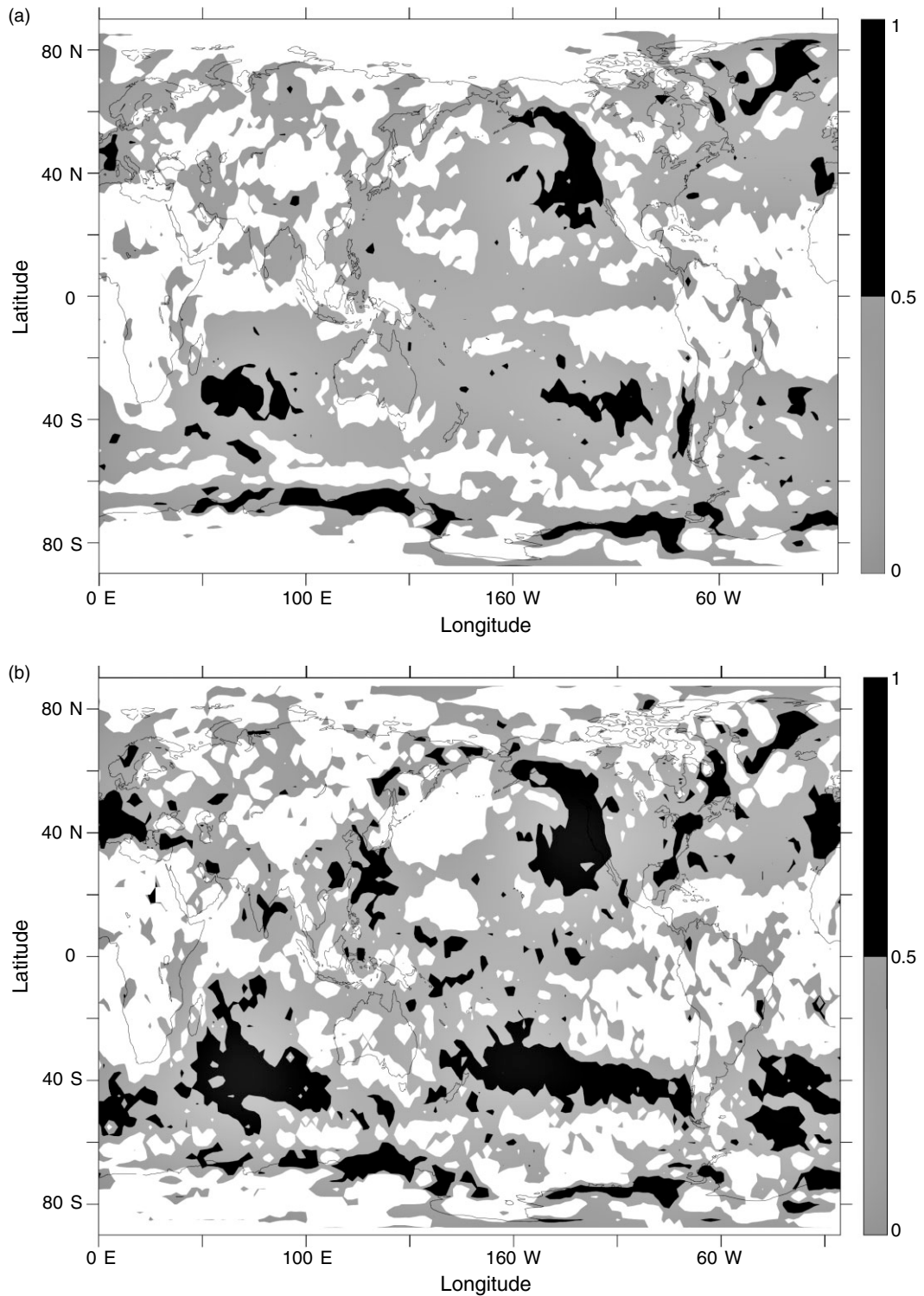


Figure 11. MSE skill score for monthly precipitation over the verification period, computed over (a) all seasons, (b) boreal winter (December–January–February), and (c) boreal summer (June–July–August). Shaded areas indicate some skill over climatology. Darker shading indicates higher skill. Clear areas have negative scores and correspond to less skill than climatology

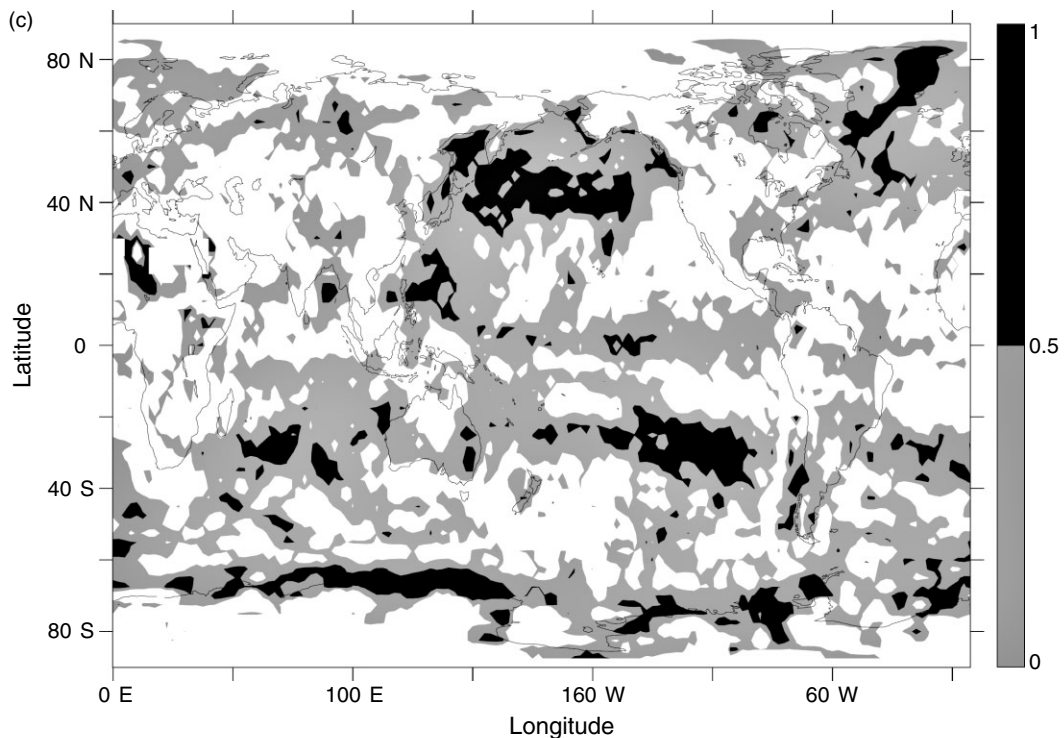


Figure 11. (Continued)

the limitations it is remarkably successful. The above results show that although the skill is widely variable throughout the globe and the seasons, generally speaking the scheme is capable of skilfully diagnosing monthly precipitation over midlatitude oceans, and over continental areas during the winter season. The anomaly correlations clearly demonstrate that higher skill is found in the midlatitudes and over the oceans. The MSE skill score maps show that, taken as a whole, the scheme is moderately skilful in midlatitudes, but when examined by season there are more clearly defined areas of high skill and no skill.

The OMEGA scheme tends to be more skilful where and when the variability of vertical motion (as measured on a 2.5 grid cell) is strongly coupled to the generation of precipitation. At this scale, the vertical motion is a measure of the synoptic-scale forcing for uplift and subsidence. Precipitation that is forced primarily by the large-scale dynamics should, therefore, correlate well with the vertical motion, and thus be diagnosed skilfully by the OMEGA scheme. On the other hand, precipitation that is driven primarily by mesoscale convection has a less well defined relationship to the wider synoptic environment. In this case the precipitation will not correlate well with the vertical motion, and any scheme that uses vertical motion as a predictor (such as OMEGA) can only at best be tuned to be unbiased over long time intervals (essentially reproducing the climatology); skilfully diagnosing month to month precipitation variability with such a scheme is difficult.

It is thus reasonable to expect the OMEGA scheme to be more skilful in the midlatitudes, where precipitation tends to be driven by synoptic-scale systems, than in the tropics, where smaller scale convection is more important. Similarly, it is reasonable that the winter season is handled more skilfully than the summer, since winter precipitation in midlatitudes is strongly governed by synoptic-scale cyclones, whereas summer-season precipitation tends to be more local and convective in nature. This conclusion of a better performance in winter was also reached by van den Dool (1987) in his study over the USA.

One salient feature on the MSE skill score maps is an area of very high skill along the west coast of North America. This part of the world is characterized by high precipitation driven by upslope flow as the prevailing westerly winds encounter the coastal ranges and the Rocky Mountains. Referring back to Figure 2,

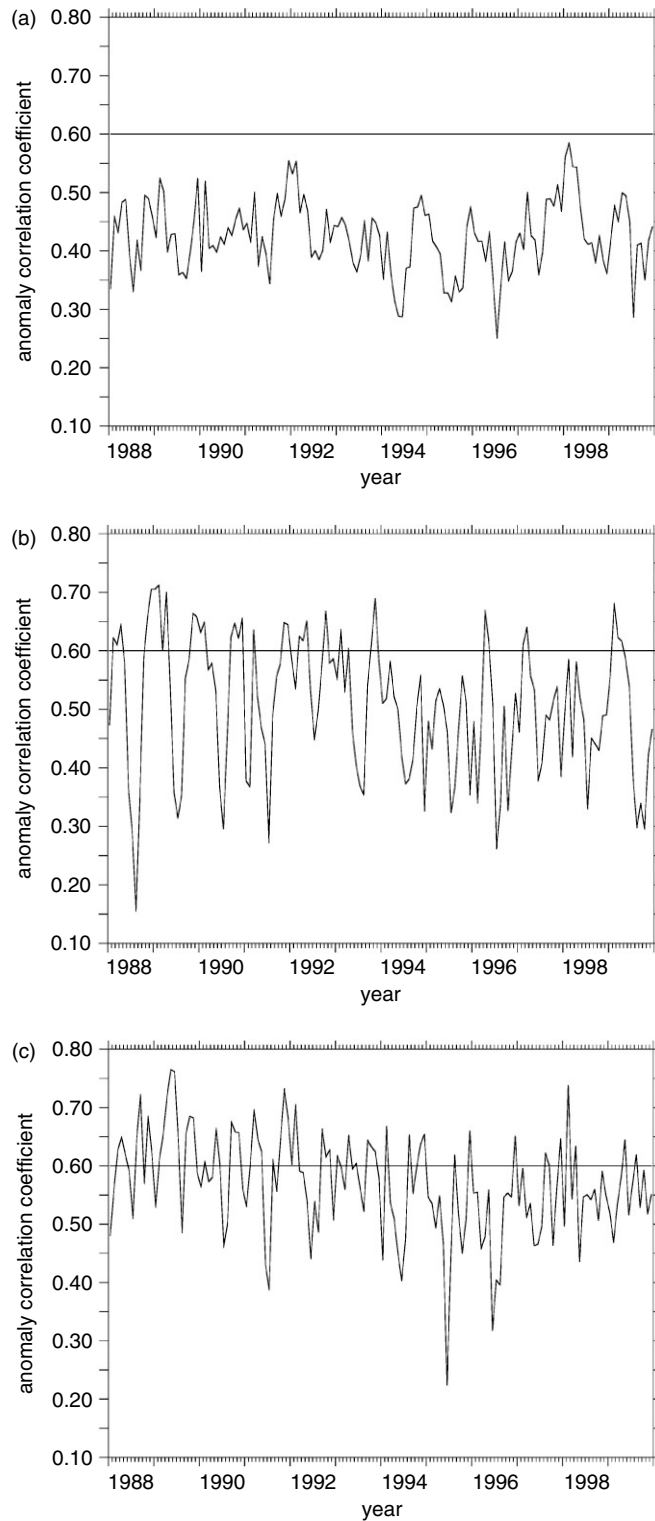


Figure 12. AC scores over the verification period, computed over (a) the whole globe, (b) northern midlatitudes (30–60 N), and (c) southern midlatitudes (30–60 S). The subjective threshold of 0.6 is included for comparison

the correlation between precipitation and vertical motion is very high in this region. The NCEP reanalysis vertical motion is therefore a good measure of the upslope flow that drives the copious rainfall along the coast of British Columbia and the Pacific Northwest of the USA.

6. DISCUSSION AND CONCLUSIONS

We have taken a simplistic approach in this study. We were interested in reducing the temporally and spatially highly variable precipitation and vertical motion fields to an elegant and easily modelled relationship. This was done in Sections 3 and 4, and we consider these to be the most significant findings. The subsequent results in Section 5 are merely an illustration of the potential of the scheme, and serve as a guide for the expected skill when the scheme is eventually applied to climate modelling and forecasting. There are many ways in which we could increase the complexity and sophistication of the predictor, and thereby reduce the error. Examples include adding other variables, such as moisture, to the regression (van den Dool, 1987), or using past values of precipitation to take advantage of the serial correlation inherent in the system. But these types of enhancement move us further away from the elegant simplicity that we sought. At any rate, it is always interesting to test the limits of the very simplest forecasting techniques before moving to more sophisticated schemes.

In Section 1 we stated that the practical goal of the project was to develop a precipitation scheme for use in a dry climate model. The OMEGA scheme was developed and tested without any reference to the eventual coupling with a GCM. A few words about the actual implementation of such a coupled model are in order. One would not want simply to couple the parameters of the OMEGA scheme (slopes and intercepts) to the vertical motion output of a GCM. The OMEGA scheme has been tuned to the vertical motion of the NCEP reanalysis. Vertical motion is not a measured variable and is sensitive to the particular vertical balance scheme used in the model; the desired GCM may produce vertical motion fields significantly different from those of the reanalysis. The OMEGA scheme should be retuned to the new model by integrating the GCM over a control period for which adequate precipitation data are available (in this study it was 1976 through to 1987), and extracting the model's vertical motion fields. Then a straightforward reapplication of the procedure in Section 4 will yield the parameters for a new OMEGA scheme properly balanced for that GCM.

Future extensions of this research are possible, both in theory and application. The last several years have witnessed an explosion of new atmospheric data products, such as reanalyses and merged precipitation analyses, and many of these data sets are being extended in near real-time. As the available data grows, so does the opportunity to test and refine the statistical relationship between precipitation and vertical motion further. In particular, the extension of the IDD precipitation data set will soon allow us to tune the precipitation scheme independently of the model-derived reanalysis precipitation fields.

On the application side, it is possible to proceed directly to the coupling of the OMEGA scheme with Hall's (2000) dry GCM. This gives a computationally very cheap method to extract precipitation fields from the model based on the simulated vertical motion, and a new tool for diagnostic climate studies. The caveat is, of course, that the scheme is empirically based on past observations, and therefore implicitly assumes a statistically stationary climate. The scheme should not be blindly applied to climate change scenarios; in fact, Hall (2000) urges a similar caution for his model, which is driven by a forcing function computed from past observations. However, for studies of variability with a steady climate, or transient responses to anomalous climate perturbations, this coupled system will provide a simple and efficient platform for numerical experimentation.

ACKNOWLEDGEMENTS

Financial support for this work was provided by the Natural Sciences and Engineering Research Council of Canada (grant 1668-00) to C.A. Lin. The use of the computational facilities of the Centre de recherche en calcul appliqué is gratefully acknowledged.

REFERENCES

- Chen QS, Bromwich DH, Bai L. 1997. Precipitation over Greenland retrieved by a dynamic method and its relation to cyclonic activity. *Journal of Climate* **10**(5): 839–870.
- Hall NMJ. 2000. A simple GCM based on dry dynamics and constant forcing. *Journal of the Atmospheric Sciences* **57**(10): 1557–1572.
- Huffman GJ, Adler RF, Arkin P, Chang A, Ferraro R, Gruber A, Janowiak J, McNab A, Rudolf B, Schneider U. 1997. The Global Precipitation Climatology Project (GPCP) combined precipitation dataset. *Bulletin of the American Meteorological Society* **78**(1): 5–20.
- Huffman GJ, Adler RF, Morrissey MM, Bolvin DT, Curtis S, Joyce R, McGavock B, Susskind J. 2001. Global precipitation at one-degree daily resolution from multisatellite observations. *Journal of Hydrometeorology* **2**(1): 36–50.
- Janowiak JE, Gruber A, Kondragunta CR, Livezey RE, Huffman GJ. 1998. A comparison of the NCEP–NCAR reanalysis precipitation and the GPCP rain gauge–satellite combined precipitation dataset with observational error considerations. *Journal of Climate* **11**: 2960–2979.
- Kalnay E, Kanamitsu M, Kistler R, Collins W, Deaven D, Gandin L, Iredell M, Sasha S, White G, Woollen J, Zhu Y, Chelliah M, Ebisuzaki W, Higgins W, Janowiak J, Mo K, Ropelewski C, Wang J, Leetmaa A, Reynolds R, Jenne R, Joseph D. 1996. The NCEP/NCAR 40-year reanalysis project. *Bulletin of the American Meteorological Society* **77**(3): 437–471.
- Sinclair MR. 1994. A diagnostic model for estimating orographic precipitation. *Journal of Applied Meteorology* **33**(10): 1163–1175.
- Van den Dool HM. 1987. An empirical study on the parameterization of precipitation in a model of the time mean atmosphere. *Journal of the Atmospheric Sciences* **44**(1): 224–235.
- Von Storch H, Zwiers FW. 1999. *Statistical Analysis in Climate Research*. Cambridge University Press: Cambridge, U.K.
- Wilks DS. 1995. *Statistical Methods in the Atmospheric Sciences*. Academic Press: San Diego.